Proc. Nat. Acad. Sci. USA
Vol. 70, No. 6, pp. 1677–1681, June 1973

Gap Junctions between Photoreceptor Cells in the Vertebrate Retina

(membranes/electron microscopy/freeze-fracturing)

ELIO RAVIOLA AND NORTON B. GILULA*

Department of Anatomy, Harvard Medical School, Boston, Massachusetts 02115

Communicated by Don W. Fawcett, March 23, 1973

ABSTRACT **In the outer plexiform layer of the retina the synaptic endings of cone cells make specialized junctions with each other and with the endings of rod cells. The ultrastructure of these interreceptor junctions is described in retinas of monkeys, rabbits, and turtles, in thin sections of embedded specimens and by the freeze-fracturing technique. Cone-to-rod junctions are ribbon-like areas of close membrane approximation. On either side of the narrowing of the intercellular space, the junctional membranes contain a row of particles located on the fracture face A (cytoplasmic leaflet), while the complementary element, a row of single depressions, is located on fracture face B. The particle rows are surrounded by a membrane region that is devoid of particulate inclusions and bears an adherent layer of dense cytoplasmic material. Cone-to-cone junctions in some places are identical to cone-to-rod junctions, while in other places they closely resemble typical gap junctions (nexus). Interreceptor junctions, therefore, represent a morphological variant of the gap junction, and probably mediate electrotonic coupling between neighboring photoreceptor cells.**

The ultrastructural analysis of the retina in several vertebrate species has shown that the synaptic endings of photoreceptor cells in the outer plexiform layer contact each other, without intervening glia, at specialized sites, marked by symmetrical layers of dense, fluffy material on the cytoplasmic aspect of the adjoining membranes, and focal membrane fusion or close approximation (1–10). These interreceptor contacts have been interpreted as synapses (1), desmosomes (2, 8), tight junctions (5), or gap junctions (10); their functional significance, however, remains obscure, primarily because their tenuous appearance in thin sections of embedded specimens does not permit a definitive statement as to their morphological identity.

In this study, we have applied to the retina the technique of freeze-fracturing (11), which provides extended views of the internal structure of the membranes (12–14) and thus permits a more precise characterization of intercellular junctions (15–20). We present evidence that in primate, lagomorph, and chelonian retinas, photoreceptor cells are connected to each other by an unusual type of gap junction or nexus. We therefore describe a structural basis for the facilitatory interaction between cone cells, which has been demonstrated by intracellular recordings in turtle retinas (21).

MATERIALS AND METHODS

The light-adapted retinas of monkeys (*Macaca mulatta* and *Macaca arctoides*), rabbits (New Zealand albino and Dutch belted), and turtles (*Pseudemys scripta elegans*) were fixed in 2% paraformaldehyde, 2.5% glutaraldehyde in 0.1 M cacodylate buffer at pH 7.3, containing 2 mg/ml of $CaCl_2$ or in 0.05 M Sörensen phosphate buffer at pH 7.3 (22). For thin sectioning, the retinas were fixed for 4 hr in the aldehyde mixture at room temperature, briefly washed in buffer alone, postfixed in 2% OsO_4, stained *en bloc* with uranyl acetate, and embedded in Epon–Araldite. To exclude the possibility that localized narrowings of the intercellular space could represent an artifact caused by aldehyde fixation, a few specimens were fixed in phosphate-buffered 2% OsO_4 and stained *en bloc* with uranyl acetate. Staining of the intercellular spaces with colloidal lanthanum (23) was also attempted, with inconsistent results. For freeze-fracturing, retinas were fixed for 20–30 min in the aldehyde mixture at room temperature, washed with buffer alone, and infiltrated for 2 hr with 20% buffered glycerol at room temperature. The retinas were frozen in liquid Freon 22 (chlorodifluoromethane), and stored in liquid nitrogen. Freeze-fracturing and platinum–carbon shadowing were performed with a Balzer's apparatus (11, 12). Replicas were cleaned in bleach. Micrographs were taken with a Jeol 100B electron microscope. Most illustrations of freeze-fractured retinas are oriented with their scleral side at the top. A correct impression of the relief is obtained by looking with the shadow direction, indicated by *circled arrows* at the lower left corner of each figure. Freeze-fracturing splits cell membranes into an inner leaflet, which remains adherent to the cytoplasm, and an outer leaflet, which separates with the intercellular cleft. Thus, two fracture faces, which complement each other in the interior of the membrane, are artificially generated. The exposed surface of the inner membrane leaflet is conventionally designated fracture face A, while the exposed surface of the outer membrane leaflet is called fracture face B.

RESULTS

(*1*) *Monkey Retina.* (*a*) *Embedded and sectioned specimens.* In the middle zone of the outer plexiform layer, occupied by the orderly array of the synaptic endings of photoreceptor cells, small surface specializations (Figs. 1 and 6) are found at the interface between neighboring cone cell endings (pedicles) or between pedicles and rod cell endings (spherules). Rarely do they occur between adjacent spherules. The fine structure of these interreceptor junctions closely conforms to the description provided by Lasansky (10) for turtle retina. The plasma membranes of the adjoining endings are in mutual contact for a short distance without intervening processes of the Müller glial cells; they are decorated on their cytoplasmic aspect with a layer of dense, fluffy material, and they approach

* Present address: The Rockefeller University, New York, N.Y. 10021.

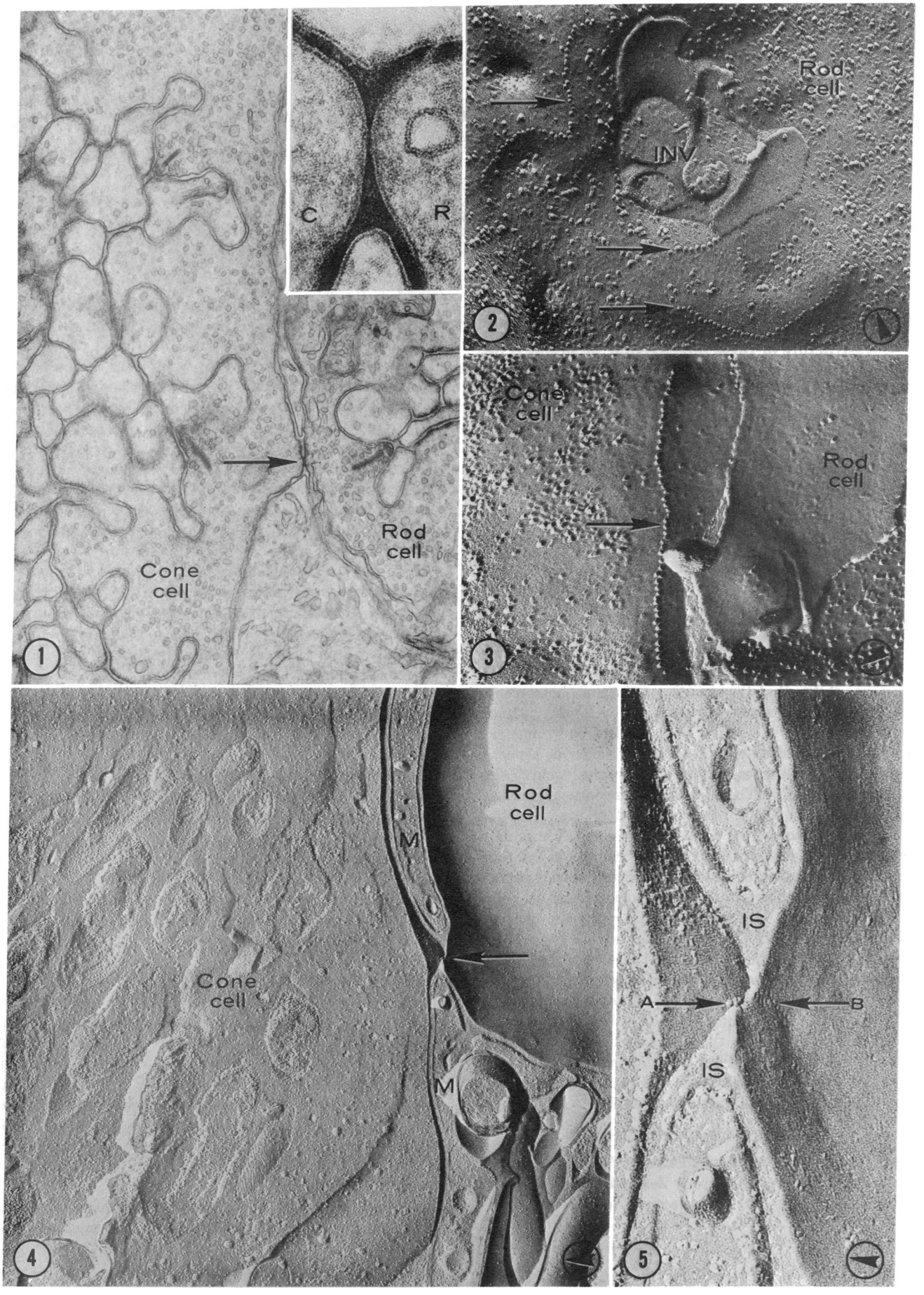

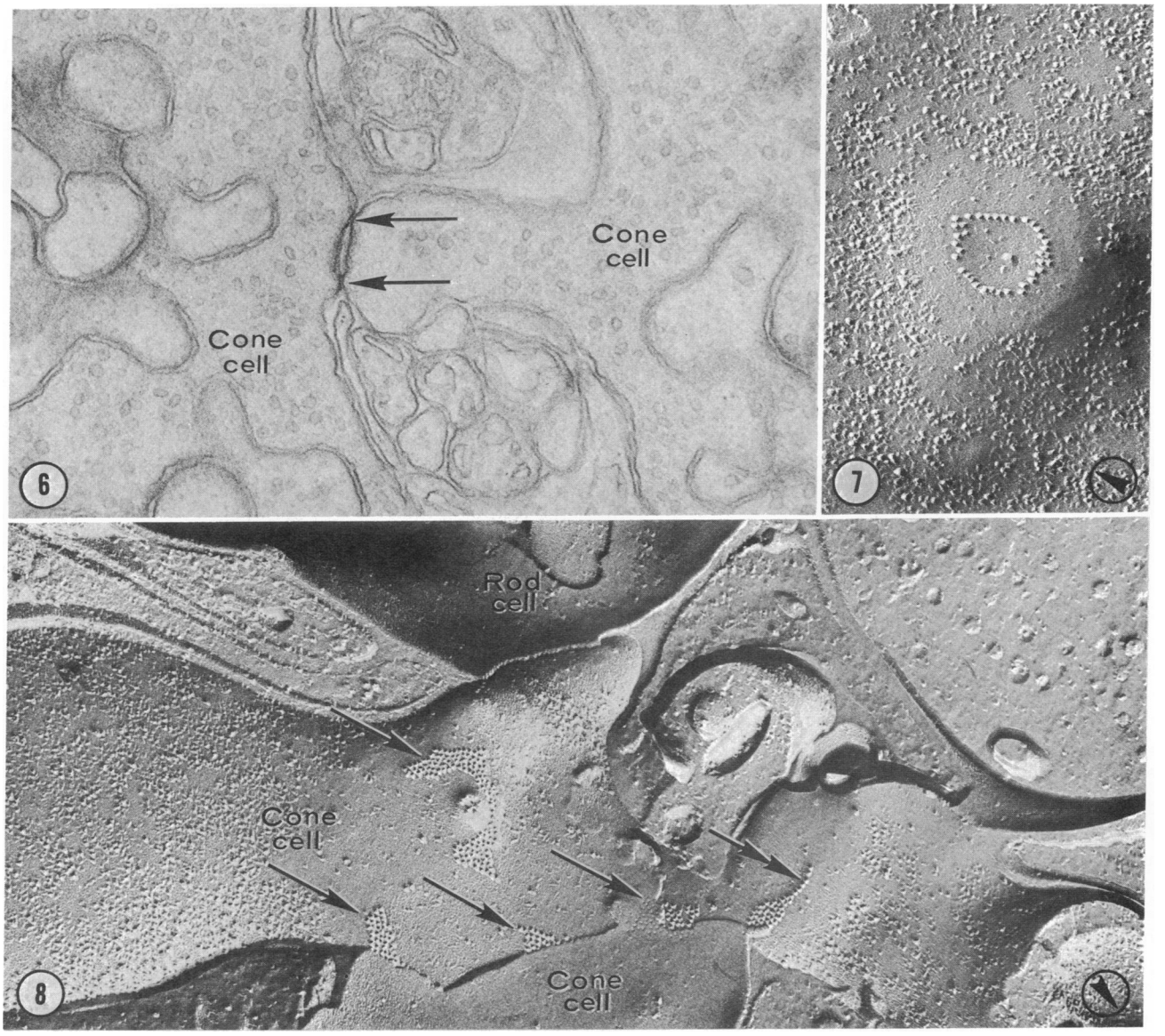

FIG. 1. Monkey retina: tangential section. A cone-to-rod junction is seen at the *arrow*. The adjoining photoreceptor cell membranes approach each other closely without intervening glia and bear a layer of dense material on their cytoplasmic aspect. Magnification: ×33,000. *Inset:* Staining with lanthanum tracer shows that membranes do not fuse at the junctional site. *C:* cone pedicle; *R:* rod spherule. Magnification: ×150,000.

FIG. 2. Monkey retina: freeze-fracture. The fracture plane has exposed the A-face of the membrane on the vitreal aspect of a rod spherule. In the center, the mouth of the synaptic invagination (*INV*) is seen, occupied by the cross section of the cell processes that synapse with the spherule. Three rows of particles are indicated (*arrows*), sitting on slight bulges of the spherule surface. Magnification: ×87,000.

FIG. 3. Monkey retina: freeze-fracture. A row of particles (*arrow*) on the A-face of a cone pedicle is surrounded by a region of membrane matrix almost devoid of particles. Magnification: ×98,000.

FIG. 4. Monkey retina: freeze-fracture. The fracture process has cut across a cone pedicle, and has exposed the B-face of the membrane of a neighboring rod spherule. The cross-fracture of two Müller cell processes (*M*) is seen between the two photoreceptor cells. The membranes of the adjoining endings approach each other closely without intervening glia (*arrow*). Magnification: ×35,000.

FIG. 5. Higher magnification of the interreceptor junction in Fig. 4. The A-face of the pedicle membrane and the B-face of the spherule membrane are seen next to each other on either side of the intercellular space (*IS*), where the two adjacent membranes come close together. Three particles are seen on the A-face of the pedicle membrane (*arrow labeled A*) and a row of pits is seen on the B-face of the spherule membrane (*arrow labeled B*). Particles and pits are in register with each other at the site of the junction. Magnification: ×145,000.

FIG. 6. Monkey retina: tangential section. Cone-to-cone junctions are often characterized by two sites of membrane approximation (*arrows*), on either side of a desmosome-like specialization. Magnification: ×55,000.

FIG. 7. Monkey retina: freeze-fracture. A circular row of particles is present on a protrusion of the surface of a pedicle. Note the conspicuous absence of particles in the surrounding matrix. This circular particle arrangement may represent the freeze-fracture appearance of the junction in Fig. 6. Magnification: ×88,000.

FIG. 8. Monkey retina: freeze-fracture. More extensive gap junctions (*arrows*) are present between a cone basal process and a neighboring pedicle. Note that one of the junctions continues as a single row of particles (*double-headed arrow*). Magnification: ×64,000.

each other focally at one or two points, almost obliterating the intercellular space. However, if the specimen is tilted with respect to the electron beam in order to compensate for membrane obliquity, a 2- to 4-nm intercellular space is consistently observed at the points of focal membrane approximation. Junctions are symmetrical, and synaptic vesicles do not congregate preferentially near the junctional membrane.

Most cone-to-rod junctions show a single spot of close membrane approximation either in the middle or at one end of the surface segment that bears the coat of dense cytoplasmic material (Fig. 1). Cone-to-cone junctions are more prominent and clearly consist of two components: (*i*) a desmosome-like portion, where cells are separated from each other by a cleft 12 nm in thickness, and (*ii*) one or two spots of close membrane approximation, typically occurring on either end of the desmosome-like segment (Fig. 6).

In the region of the foveal slope, where rod spherules are lacking, cone-to-cone junctions are found either at the circumference of the pedicles or between their scleral surface and neighboring inner cone fibers. We were unable to establish whether specialized contacts were also present between the pedicles that belong to the bouquet of central cones. In the rest of the central area, junctions occur along the lateral surface of cone pedicles, whereas in the retinal periphery they are commonly found either along or at the tip of cone basal processes. In tangential sections through the outer plexiform layer, pedicles seem to contact indiscriminately all adjoining endings. The staining of the intercellular clefts with lanthanum tracer confirms that photoreceptor cell membranes do not fuse at the site of the junction (Fig. 1, *inset*).

(*b*) *Freeze-fracturing.* In replicas of freeze-fractured monkey retinas, spherules are easily recognized from pedicles by their small size, rounded shape, and the presence of a single invagination occupied by horizontal and bipolar cell processes. When the fracture plane exposes the vitreal aspect of the spherule by removing the outer portion of the membrane, one to four remarkable A fracture face specializations are seen at a short distance from the depression that leads into the synaptic invagination (Fig. 2): each specialization consists of a linear array of intramembrane particles, which is located at the summit of a small ridge almost devoid of intramembrane inclusions. The particle arrays are scattered at irregular intervals from each other, and they are never organized into a continuous belt or zonula, which encircles the synaptic invagination. Each array usually consists of some 50 particles arranged in a single row, 0.4–0.6 μm in length; the row is straight, curved, or angular, and rarely branched. In some places, however, the particle array is comprised of two closely adjacent rows, slightly out of register with respect to each other. Individual particles have a diameter of 8–14 nm, and in places show a small apical depression; their center-to-center spacing varies from 8 to 18 nm. On the fracture face B of the spherule membrane, the A-face specialization is complemented by a row of irregularly spaced pits or depressions, which are located at the bottom of a shallow groove devoid of intramembrane inclusions. Since the junctional particles are consistently present on the A-face, the variation in their center-to-center spacing cannot reflect unequal particle dispositions between the two fracture faces.

On the A-face of the membrane of cone pedicles and along their basal processes, the junctional membrane pleomorphism is more apparent than on the rod spherules. Linear arrays of particles are fairly common (Fig. 3). In some cases, the ends of the linear particle arrays may join to form a complete circle (Fig. 7). In still other cases, some 30–50 particles occur in hexagonally packed aggregates (Fig. 8), essentially identical to the A-face appearance of the vertebrate freeze-fractured gap junction or nexus (15, 17–20). These aggregates, however, are frequently continuous with a short segment of a linear array of particles. The A-face specialization of pedicles is also complemented by arrays of pits on the B-face, and the membrane specialization is surrounded by a region almost devoid of particles on both fracture faces.

In order to precisely relate the intramembrane specializations exposed by freeze-fracturing to the interreceptor junctions seen in thin sections, it is necessary to obtain slightly cross-fractured images of the contact region that contain the same structural information present in thin sections. Fig. 4 is a representative image of such a cross fracture, which permits both the positive identification of two adjacent photoreceptor cells, as well as the exact site of the interreceptor junction. At this cone-to-rod junction, the interiors of both membranes are exposed on either side of the cross-fractured intercellular space. The A-face particle row of one junctional membrane lies in perfect register with the row of B-face pits of the adjacent membrane (Fig. 5), and both membrane differentiations face each other across an abrupt narrowing of the intercellular cleft. This is the site where the photoreceptor cell surfaces approach each other closely without intervening glia. Thus, the intramembrane specializations at the cone-to-rod interface truly represent the freeze-fracture counterpart of the junction as seen in thin-sectioned specimens, and the cone-to-rod junction can be described as follows: (*a*) it is a narrow band of close membrane approximation; (*b*) it is characterized by a symmetrical arrangement of intramembrane particle rows; and (*c*) it is surrounded by a region that is almost devoid of particulate inclusions within the plane of the membrane, and bears an adherent layer of dense cytoplasmic material.

On the basis of similar evidence, it appears that cone-to-cone junctions in some places are identical to cone-to-rod junctions, while in other places they more closely resemble the typical gap junction. Furthermore, those junctions that are characterized in thin sections by two spots of focal membrane approximation on either side of a desmosome-like specialization, may actually represent curved or circular junctions, containing a ring of particles embedded in both adjoining photoreceptor cell membranes.

In replicas of the peripheral monkey retina, where most of the interreceptor junctions occur along the cone basal processes, it is very difficult to trace a surface specialization to its parent ending. We can deduce, however, that all linear aggregates of particles found in the outer plexiform layer belong to interreceptor junctions; for no comparable arrangement of particles is found at specialized contacts involving bipolar, horizontal, and Müller glial cells.

(*2*) *Rabbit Retina.* Cone cell pedicles in the rabbit retina are provided with a profusion of basal processes, which establish specialized contacts with neighboring pedicles and spherules. In thin sections, the interreceptor junctions do not differ significantly from those described in the primate retina. In freeze-fracture replicas, only cone-to-rod junctions were identified thus far, and they appear identical to the linear junctions in monkeys.

(*3*) *Turtle Retina.* Cone-to-cone junctions present in turtle retinas are also characterized by a row of intramembrane A-face particles.

DISCUSSION

Interreceptor junctions share two essential features with the gap junction: (*i*) the adjacent cell membranes are closely apposed but not fused (23), and (*ii*) the membranes contain symmetrical arrays of homogeneous particle aggregates on their fracture face A (15, 17–20) at the site of close apposition. Further, these junctions possess a pleomorphism that ranges from the planar hexagonal lattice typical of gap junctions (cone-to-cone) to a single linear aggregate (cone-to-rod). Lasansky's hypothesis of gap junctions (10) is therefore substantiated by this study, and the possibility is ruled out that interreceptor junctions could represent synapses (1), mere attachment devices (2, 8), or tight junctions (5).

There is now considerable evidence that gap junctions represent a pathway for intercellular communication (see ref. 24); thus, cone cells are likely to be electrically coupled to each other and to neighboring rod cells. However, direct experimental evidence to support this hypothesis is only available for turtle cone cells (21). On the other hand, the strategic location of interreceptor junctions at the synaptic endings, far removed from the cell region involved in stimulus processing, rules out the possibility that they might only subserve some sort of metabolic cooperation (24) between photoreceptor cells. Moreover, their widespread occurrence in vertebrate retinas suggests that they have a basic role in the process of encoding visual information.

The unusual organization of interreceptor nexus raises several considerations. Their pleomorphism suggests that the geometrical arrangement of particles within the plane of the membrane may only be of secondary functional importance in intercellular communication. In fact, if the linear junctions represent functional intercellular pathways, then polygonal packing is definitely not a requirement for functional viability. Also, tenuous linear structures such as these may represent a form of the gap junction that is capable of undergoing a rapid transformation from functional to nonfunctional. Their close association with a desmosomal component suggests that some mechanical anchoring may be necessary to maintain the sets of gap junctional channels in register. This device m ght be very important since the junctions are so small.

This study provides the structural basis for a short-range transfer of electrical events from cones to neighboring rods and cones, and from many rods onto a central cone. The possibility that interconnections are confined within specific cone mechanisms, as suggested by the selective spreading of facilitation among turtle cone cells (21), cannot be ruled out, but on morphological grounds it seems unlikely. Previous studies (6, 7), as well as our own, show that in mammalian retinas the distribution of interreceptor junctions is indiscriminate, at least within the limits of the small areas of the outer plexiform layer that can be analyzed with an electron microscope. The functional significance of this "spilling over" of signals throughout the retina, and the manner in which it is exploited by subsequent neuronal networks is unknown. The existence of interreceptor gap junctions, however, would seem to weaken the widespread concept that retinal photoreceptors represent a mosaic of independent units in which the visual world evokes a point-to-point representation.

1. Sjöstrand, F. S. (1958) *J. Ultrastruct. Res.* **2**, 122–170.
2. Missotten, L., Appelmans, M. & Michiels, J. (1963) *Bull. Mém. Soc. Fr. Ophtalmol.* **76**, 59–82.
3. Cohen, A. I. (1964) *Invest. Ophthalmol.* **3**, 198–216.
4. Cohen, A. I. (1965) *J. Anat.* **99**, 595–610.
5. Dowling, J. E. & Boycott, B. B. (1966) *Proc. Roy. Soc. Ser. B* **166**, 80–111.
6. Cohen, A. I. (1969) "The retina", in *UCLA Forum in Medical Sciences No. 8*, eds. Straatsma, B. R., Hall, M. O., Allen, R. A. & Crescitelli, F. (University of California Press, Berkeley, Calif.), pp. 31–62.
7. Sjöstrand, F. S. (1969) "The retina," in *UCLA Forum in Medical Sciences No. 8*, eds. Straatsma, B. R., Hall, M. O., Allen, R. A. & Crescitelli, F. (University of California Press, Berkeley, Calif.), pp. 63–100.
8. Dowling, J. E. (1970) *Invest. Ophthalmol.* **9**, 655–680.
9. Lasansky, A. (1971) *Phil. Trans. Roy. Soc. London Ser. B* **262**, 365–381.
10. Lasansky, A. (1972) *Invest. Ophthalmol.* **11**, 265–275.
11. Moor, H., Mühlethaler, K., Waldner, H. & Frey-Wyssling, A. (1961) *J. Biophys. Biochem. Cytol.* **10**, 1–14.
12. Branton, D. (1966) *Proc. Nat. Acad. Sci. USA* **55**, 1048–1056.
13. Pinto da Silva, P. & Branton, D. (1970) *J. Cell. Biol.* **45**, 598–605.
14. Tillack, T. W. & Marchesi, V. T. (1970) *J. Cell Biol.* **45**, 649–653.
15. Kreutziger, G. O. (1968) in *26th Proceedings Electron Microscopy Society of America* (Claitor's Publishing Division, Baton Rouge, La.), pp. 234–235.
16. Staehelin, L. A., Mukherjee, T. M. & Williams, A. W. (1969) *Protoplasma* **67**, 165–184.
17. Goodenough, D. A. & Revel, J. P. (1970) *J. Cell Biol.* **45**, 272–290.
18. Chalcroft, J. P. & Bullivant, S. (1970) *J. Cell Biol.* **47**, 49–60.
19. McNutt, N. S. & Weinstein, R. S. (1970) *J. Cell Biol.* **47**, 666–688.
20. Friend, D. S. & Gilula, N. B. (1972) *J. Cell Biol.* **53**, 758–776.
21. Baylor, D. A., Fuortes, M. G. F. & O'Bryan, P. M. (1971) *J. Physiol.* **214**, 265–294.
22. Karnovsky, M. J. (1965) *J. Cell Biol.* **27**, 137 abstr.
23. Revel, J. P. & Karnovsky, M. J. (1967) *J. Cell. Biol.* **33**, C7–C12.
24. Gilula, N. B., Reeves, O. R. & Steinbach, A. (1972) *Nature* **235**, 262–265.